**Supporting Information for**

**A Graphene-Based Affinity Nanosensor for Detection of Low-Charge and Low-Molecular-Weight Molecules**

Yibo Zhu, Yufeng Hao, Enoch Adogla, Jing Yan, Junyi Shang, Dachao Li, Kexin Xu,
Qian Wang, James Hone, and Qiao Lin

**Chemical and Materials:** The stock glucose solution (25 mM) was made by dissolving D-(+)-Glucose monohydrate (Sigma-Aldrich, #49159) in buffer. Desired concentrations were obtained by further diluting the stock solution using the same buffer. The ionic strength of the buffer was adjusted to ~10 mM by diluting the standard Dulbecco's phosphate-buffered saline (Thermo Fisher Scientific, #14190-144) using deionized water (Ricca Chemical, #9150). Reduction of the ionic concentration in the solution increased the Debye length of the electrical double layer (EDL) and decreased the capacitance of EDL capacitor. This would as a result allow the transfer characteristics to shift more significantly given a specific doping in graphene. The pH levels of the diluted PBS, as well as the glucose solutions were measured to be 7.4 ± 0.05 (n=3). Pyrene-1-boronic acid (PBA, Sigma-Aldrich, #542873) was dissolved in acetonitrile (Sigma-Aldrich, #271004) to obtain 0.1 mM solution for graphene functionalization. Graphene was grown on copper foil via chemical vapor deposition (CVD) in a tube furnace following an established protocol [S1].

**Fabrication:** The device was fabricated using micro and nanofabrication techniques on a silicon wafer with 285 nm wet thermal grown oxide. The substrate was washed using acetone, isopropanol (IPA) and deionized (DI) water sequentially and then further cleaned using reactive oxygen plasma to remove tiny organic residue. Graphene grown on Cu foil was cut into 3 mm by 3 mm and transferred onto the substrate using floating transfer method [S2]. Photolithography, with a bilayer resist (LOR and S1811), was used to pattern the source and drain electrodes, which were then metallized using electron beam evaporator (Angstrom EvoVac, 5/20/20 nm Cr/Pd/Au). Lift-off was completed by rinsing the chip in Remover PG and then gently washed using IPA and DI water. The graphene was then patterned to be a rectangular channel (typically 20 μm by 30 μm) using photolithography and reactive oxygen etching. The chip was then again rinsed in Remover PG, IPA and DI water, gently blow dried using compressed nitrogen, and stored in vacuum before tests.

**CVD graphene synthesis:** In this work, we used an established chemical vapor deposition (CVD) method that yields predominantly single-layer graphene (> 97% of graphene grown on Cu), as reported in prior works[1, 2]. Also, additional graphene layers beyond the single layer, if any, typically appear as small grains in isolated local regions, and can be easily identified on the basis of the brightness and contrast under an optical microscope when transferred onto a 285 nm thick $SiO_2$ coated silicon substrate (Figure S1). In our experiments, the graphene used to fabricate the conducting channel (Figure 1b) was carefully selected from the graphene transferred on the substrate to ensure the uniformity of single-layer graphene. Furthermore, Raman spectroscopy, a most widely used method, is used to characterize the layer number of graphene. The characteristics of Raman spectra from our graphene samples were in excellent agreement with that of single-layer graphene reported elsewhere[3-5]. Thus, it is believed that the graphene in our work was single layer graphene.
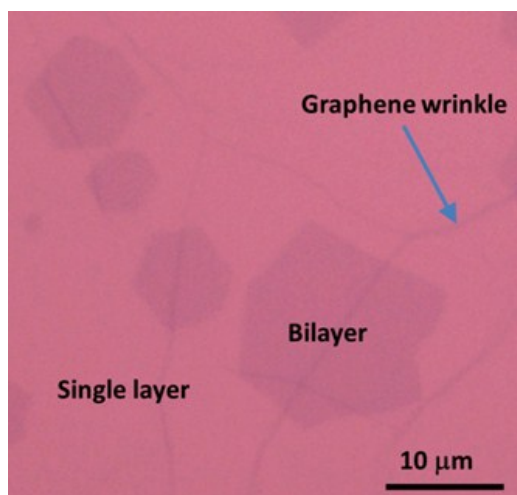
Figure S1. Microscope photo of a specifically selected local area of CVD grown graphene transferred on SiO$_2$ substrate.

**Characterization and Measurements:** The graphene transferred on the substrate was firstly inspected using optical microscope and then characterized using Raman spectroscopy (Renishaw inVia micro-Raman, excitation laser wavelength 532 nm). The Raman spectroscope was calibrated on a clean SiO$_2$/Si substrate before and after graphene characterization. The electrical measurements of transfer characteristics were performed using two Keithley 2400 sourcemeters under control of LabVIEW programs. The transfer characteristics of the device was obtained by measuring the source-drain current ($I_{DS}$) while sweeping the gate voltage ($V_{GS}$) in a range of interest. In glucose measurements, the step for gate voltage sweeping was 25 mV. The current was allowed to stabilize for ~5 seconds before changing the gate voltage.

The Raman spectra were measured at multiple positions on the graphene sample. D-band around 1350 cm$^{-1}$ was not observed at majority of the sample, although we did observe D-band at some positions (Figure S2a), which can serve as an indication of defects in the graphene. To confirm that boronic acid was coupled to graphene via pyrene-graphene $\pi$-$\pi$ interaction, but not due to reaction of boronic acid and other chemical groups in graphene, we investigated the source of D-band. Indeed, we found the D-band well correlated to the presence of organic residues or contaminants from the fabrication process (Figure S2a-c), which were not expected to influence glucose measurements, as detailed below.

A graphene sample was, sequentially, transferred onto a SiO$_2$-coated substrate, exposed to 1 mM boric acid aqueous solution, and exposure to 1 mM PBA acetonitrile solution. Raman spectra was respectively taken of the graphene sample after each of these treatment steps. The Raman spectra remained the same before (Figure S2a) and after (Figure S2b) exposure to boric acid, without displaying any peaks indicative of boric acid even at sample positions exhibiting a pronounced D-band. This implied that boric acid did not attach to graphene without other functional groups. In contrast, after exposure to PBA, the spectra (Figure S2c) exhibited peaks that are attributable to B-O stretching, BOH bending, and $\pi$-$\pi$ interaction, respectively. These results confirm that, in our experiments, the boronic acid was coupled to graphene via $\pi$-$\pi$ interaction of pyrene and graphene.
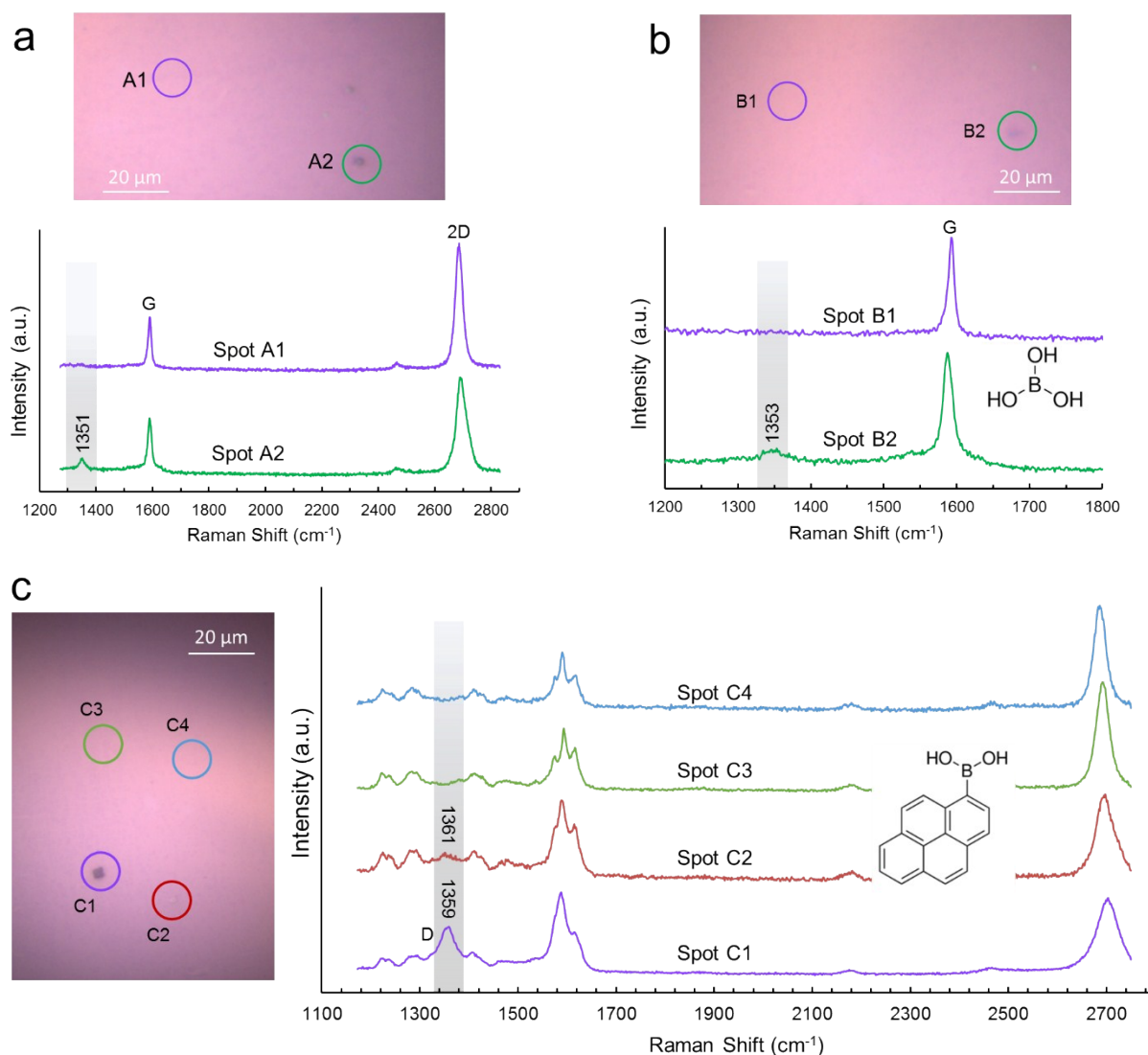
Figure S2. Characterization of graphene using Raman spectroscopy (a) after graphene was transferred onto $SiO_2$ substrate, (b) after immersing in 1 mM boric acid solution, (c) after immersing in 1 mM PBA solution.

**Influence of solution replenishment on transfer characteristics measurements:** To investigate the potential interruption of the PBA-graphene coupling by replenishment of sample solution during the nanosensor testing, we measured the transfer characteristics of PBA-functionalized graphene with fresh buffer solution added to, removed from, and then added again to nanosensor. In the two measurements when fresh buffer was added to the device, the source-drain current at each gate voltage as well as the neutral point voltage were coincident within ~1.5% (Figure S3), implying that the influence of the solution replenishment was negligible. It is thus believed that any significant response in the subsequent measurements would be attributable to the glucose-boronic acid binding.
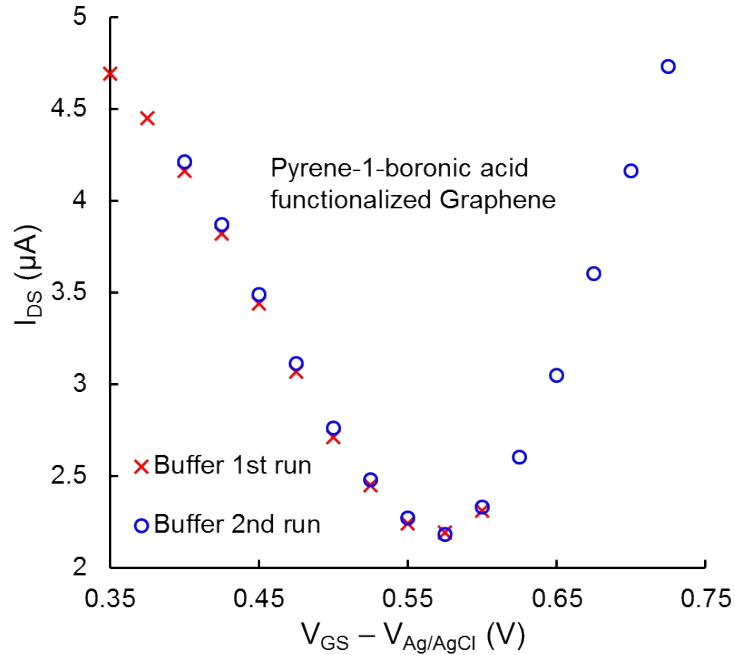
Figure S3. Influence of solution replenishment on transfer characteristics measurements. In the two measurements when fresh buffer was added to the device, the source-drain current at each gate voltage as well as the neutral point voltage were highly coincident.

**Data fitting**: The measured $\Delta V_{NP,G}/\Delta V_{NP,B}$ ratio was fitted to the Hill-Langmuir equation (Figure 4),

$$\frac{\Delta V_{NP,G}(c)}{\Delta V_{NP,B}} = A\frac{\left(\dfrac{c}{K_D}\right)^n}{1 + \left(\dfrac{c}{K_D}\right)^n} + A_0$$

where $A$ is the sensor saturation response when all boronic acid sites are occupied, $c$ is the glucose concentration, $A_0$ is an offset that accounts for the response to the fresh buffer, $K_D$ is the dissociation constant for the glucose and boronic acid binding, and $n$ is the Hill coefficient describing the binding cooperativity. A best fitting yields a $K_D$ of 38.6 µM, $A$ of 0.538, $A_0$ of -0.0037 and $n$ of 0.345.

**Measurements of glucose using butyric acid:** Moreover, we functionalized graphene with 1-pyrene-butyric acid (Sigma-Aldrich, #257354), which did not contain boronic acid (Figure S4a). We then made measurements at varying glucose concentrations on the butyric acid functionalized graphene. The measured transfer characteristics were highly coincident (Figure S4b), suggesting that there was no significant interaction of glucose and butyric acid, and that the replenishment of the sample solution did not significantly impact the transfer characteristics measurement.
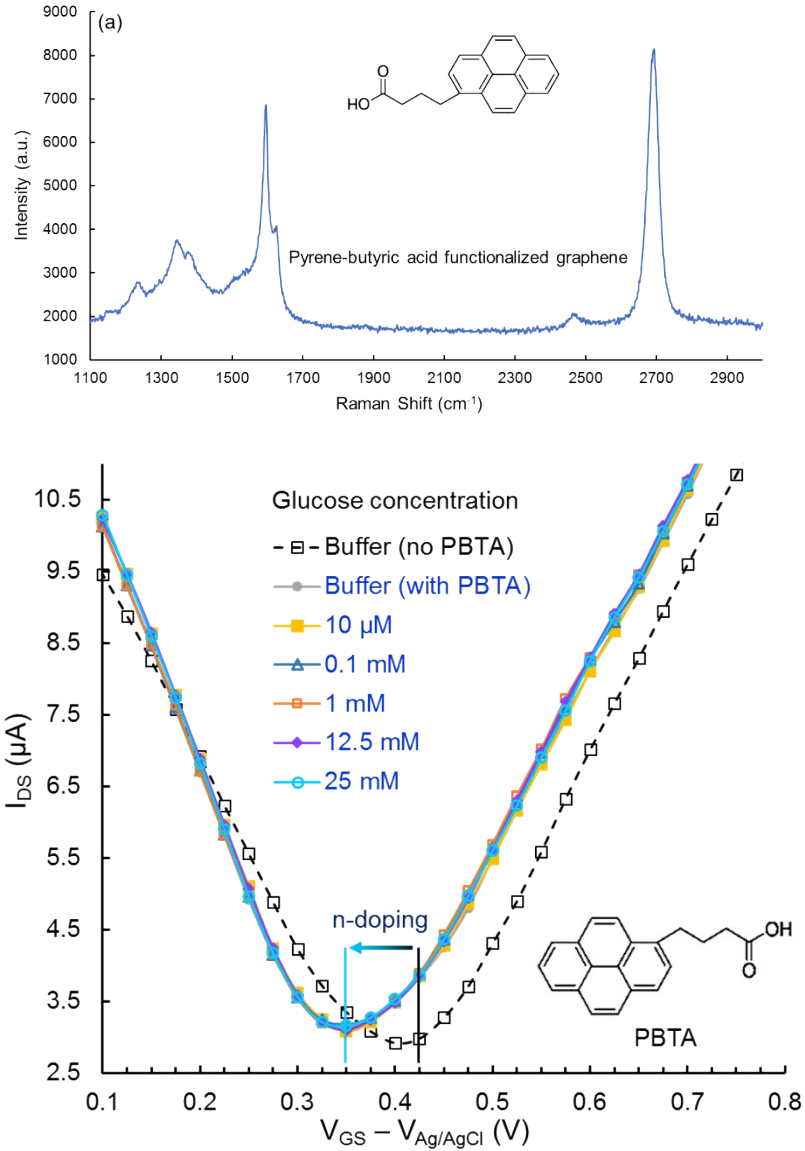
**Figure S4**. Measurements with butyric acid functionalized graphene. (a) Raman spectrum of 1-pyrene-butyric acid functionalized graphene. G-band splitting was observed, implying the molecules were coupled to graphene. (b) Transfer characteristics measured with glucose solutions on the butyric acid functionalized graphene. The n-type doping induced by PBTA remained unchanged when the sensor was exposed to glucose.

**Interpretation of transfer characteristics:** In the transfer characteristics of a field effect transistor, the source-drain current ($I_{DS}$) is roughly related to the gate voltage ($V_{GS}$) at a constant source-drain bias ($V_{DS}$) by the equation

$$I_{DS} = \mu C V_{DS}\frac{w}{l}(V_{GS} - V_{NP})$$

where $\mu$ is the graphene carrier mobility, $C$ is the gate capacitance, provided by the double layer capacitor in a solution gated GFET, $w$ and $l$ are respectively the width and length of the graphene conducting channel, $V_{NP}$ is the

neutral point voltage, representing the carrier concentration, doping level or the Fermi level relative to the Dirac point of the graphene. Taking derivative of $I_{DS}$ with respect to $V_{GS}$ ($\partial I_{DS}/\partial V_{GS}$) yields the transconductance $g_m=\mu V_{DS}Cw/l$. In Figure 3, the transconductance does not change significantly with glucose concentrations. As the gate capacitance ($C$) as well as the width ($w$) and length ($l$) of the conducting channel were not changed, the carrier mobility was believed to be constant.

**Measurements of fructose using 9-anthracene-boronic acid (ABA)**
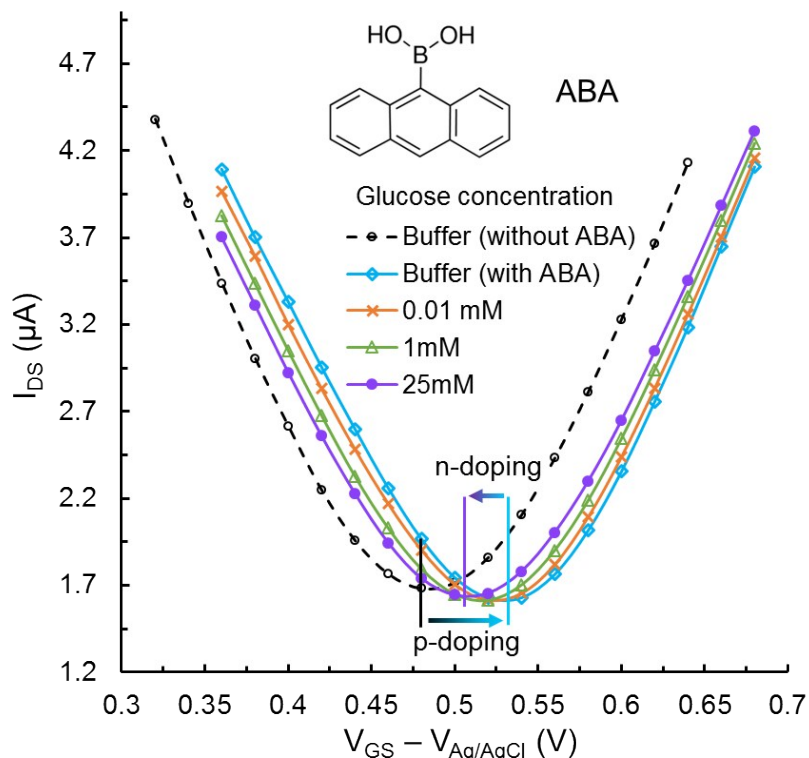


Figure **S5**. Measurements of fructose using 9-anthracene-boronic acid (ABA) as receptor. The p-doping induced by boronic acid, and the n-doping upon glucose binding were qualitatively consistent with the observations in glucose measurements using PBA.

**Measurements of fructose using PBA:**
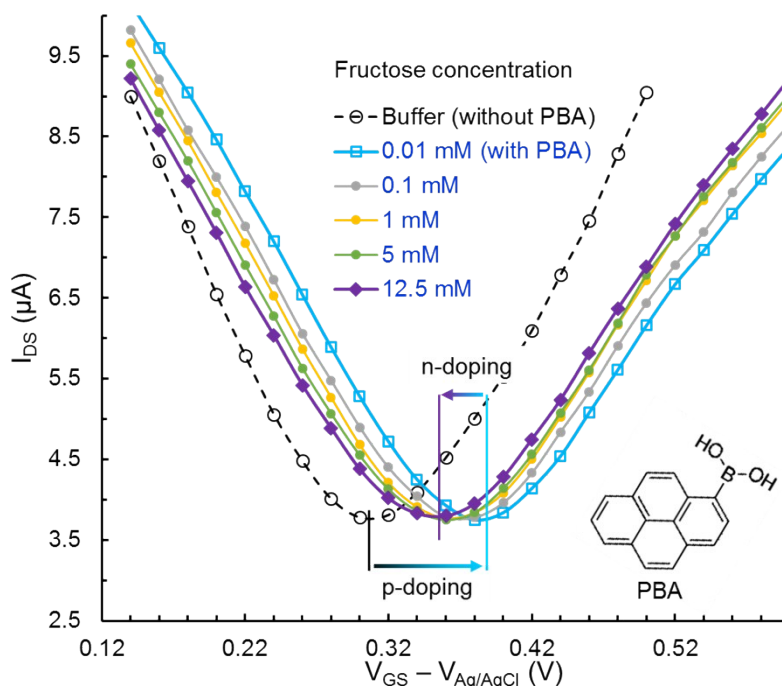


**Figure S6**. Measurements of fructose using PBA as receptor. The p-doping induced by boronic acid, and the n-doping upon glucose binding were comparable to the observations in glucose measurements.

1. X. S. Li, W. W. Cai, J. H. An, S. Kim, J. Nah, D. X. Yang, R. Piner, A. Velamakanni, I. Jung, E. Tutuc, S. K. Banerjee, L. Colombo and R. S. Ruoff, *Science*, 2009, **324**, 1312-1314.
2. Y. F. Hao, M. S. Bharathi, L. Wang, Y. Y. Liu, H. Chen, S. Nie, X. H. Wang, H. Chou, C. Tan, B. Fallahazad, H. Ramanarayan, C. W. Magnuson, E. Tutuc, B. I. Yakobson, K. F. McCarty, Y. W. Zhang, P. Kim, J. Hone, L. Colombo and R. S. Ruoff, *Science*, 2013, **342**, 720-723.
3. A. C. Ferrari, J. C. Meyer, V. Scardaci, C. Casiraghi, M. Lazzeri, F. Mauri, S. Piscanec, D. Jiang, K. S. Novoselov, S. Roth and A. K. Geim, *Phys Rev Lett*, 2006, **97**.
4. Y. F. Hao, Y. Y. Wang, L. Wang, Z. H. Ni, Z. Q. Wang, R. Wang, C. K. Koo, Z. X. Shen and J. T. L. Thong, *Small*, 2010, **6**, 195-200.
5. Z. Z. Sun, Z. Yan, J. Yao, E. Beitler, Y. Zhu and J. M. Tour, *Nature*, 2010, **468**, 549-552.